Hindawi Publishing Corporation
Mathematical Problems in Engineering
Volume 2015, Article ID 194568, 10 pages
http://dx.doi.org/10.1155/2015/194568

Research Article

Improvement on Load-Induced Cascading Failure in Asymmetrical Interdependent Networks: Modeling and Analysis

Haiyan Han and Rennong Yang

School of Aeronautics and Astronautics Engineering, Air Force Engineering University, Xi'an 710038, China

Correspondence should be addressed to Haiyan Han; hanhaiyan03@126.com

Received 2 June 2015; Revised 1 August 2015; Accepted 4 August 2015

Academic Editor: Xiaobo Qu

Many real-world systems can be depicted as interdependent networks and they usually show an obvious property of asymmetry. Furthermore, node or edge failure can trigger load redistribution which leads to a cascade of failure in the whole network. In order to deeply investigate the load-induced cascading failure, firstly, an asymmetrical model of interdependent network consisting of a hierarchical weighted network and a WS small-world network is constructed. Secondly, an improved "load-capacity" model is applied for node failure and edge failure, respectively, followed by a series of simulations of cascading failure over networks in both interdependent and isolated statuses. The simulation results prove that the robustness in isolated network changes more promptly than that in the interdependent one. Network robustness is positively related to "capacity," but negatively related to "load." The hierarchical weight structure in the subnetwork leads to a "plateau" phenomenon in the progress of cascading failure.

1. Introduction

Complex network theory has been a successful tool in modeling and analysis of modern systems [1]. A variety of network models have been proposed to approximate realistic systems such as power grids [2], transportation systems [3], communication networks [4], and other systems. Most of them focus on single and isolated systems. Recently, *interdependent network* [5] provides a new insight in understanding the structure [6], percolation [7], spreading processes [8], evolution games [9], and robustness [10, 11] of complex systems. This kind of structure usually consists of two or more subnetworks, with the subnetworks working dependently on each other [12, 13]. For example, power grids and computer systems must depend on each other because computers require power grids to supply electricity. Power grids, in turn, rely on computer systems to control power transmission process.

In 2010, Buldyrev et al. [14] found that interdependent networks have become significantly more vulnerable than their noninteracting counterparts under random attack. Gao et al. [5] reviewed the connectivity properties of "networks of networks" formed by interdependent random networks. Hu et al. [15] constructed a partially coupled network with both interdependent and interconnecting links. The interconnections satisfy "one to one" condition. They found that the change of interconnecting links leads to the change of the phase transition from second order to first order through hybrid phase transition. Huang et al. [16] studied the robustness of interdependent networks under targeted attack on high or low degree nodes. It provided a routine method to study the degree-based targeted attack problems in both single networks with dependency links [17, 18] and other general randomly connected and uncorrelated interdependent networks. Moreover, Parshani et al. [19] described the dynamic process of cascading failures on two partially interdependent networks.

Currently, researchers focus on the problem of modelling an interdependent network model for analyzing the progress of cascading failure. Based on classical network models such as ER [20], WS [21], and BA [22], researchers studied well some symmetrical and asymmetrical networks [19, 23, 24], such as ER-ER, WS-WS, BA-BA, ER-WS, BA-ER, and BA-WS; but these models differ greatly from real-world systems [25, 26]. Taking interdependent networks like ground transportation network and airline network as an example, ground

transportation network displays a hierarchical property. That is, stations at provincial level have higher capacity and more importance than municipal stations. However, the airline network can be seen as a single level network with small world property [27]. So, some other researchers [28–30] made their trials to construct framework of asymmetrical interdependent networks which are more authentic to reality.

Moreover, load such as cargoes transported in the transportation network and electric stream in power grids can trigger cascading failures [31]. The load carried by the failed nodes or edges will not disappear but will flow to the remaining part of the network, which, in a possible way, will cause further failures. As far as we are concerned, not enough attention has been paid to the cascading failure induced by load redistribution in interdependent networks.

In order to investigate the load-induced cascading failure in interdependent networks, we propose asymmetrical interdependent networks model in Section 2 and the load-induced cascading failure model in Section 3. Section 4 simulates the cascading failure in the proposed model and compares it with a WS-WS symmetrical network when nodes and edges suffer from intentional attacks, respectively. Section 5 summarizes the contribution of this paper and identifies future research needs.

2. Network Model

Figure 1 shows an asymmetrical interdependent network model. Network$_A$ has a hierarchical and weighted structure, where nodes are assigned with weights and distributed into different levels, where Network$_B$ is a single level network. The numbers of nodes in Network$_A$ and Network$_B$ are equal. The coupling proportion is set to p_1. Nodes in different subnetworks randomly construct "one to one" connections; for example, node i_A in Network$_A$ merely couples with j_B in Network$_B$.

The model can be described mathematically by $G(N, E, W)$, where $N = N_A + N_B$ is the set of nodes from Network$_A$ and Network$_B$. $E = E_A + E_B + E_{AB}$ denotes the set of edges, where E_A (E_B) denotes the internal edges of Network$_A$ (Network$_B$) and E_{AB} represents the coupling edges between the two subnetworks. Matrix $W = \begin{bmatrix} W_A & W_{AB} \\ W_{AB}^T & W_B \end{bmatrix}$ represents the adjacency matrix, where W_A and W_B represent the connections inside Network$_A$ and Network$_B$, respectively, while W_{AB} is the coupling adjacency matrix. The element ω_{ij} of W represents the weight of connection between two neighboring nodes i and j. Node intensity s_i is defined to represent the total weights of all edges connected with node i:

$$s_i = \sum_{j \in \Gamma_i} \omega_{ij}, \tag{1}$$

where Γ_i is the neighborhood of node i, including neighboring nodes in both Network$_A$ and Network$_B$.

As mentioned before, in Network$_A$, nodes are divided into several levels. There are H levels in Network$_A$ and each node from a certain level has M subordinate nodes from the next level. There are no connections between subordinate nodes in the same level except for the top level, where all nodes are connected with each other. Internal edges connecting different levels have diverse weights representing the difference in importance of interlevel connections.

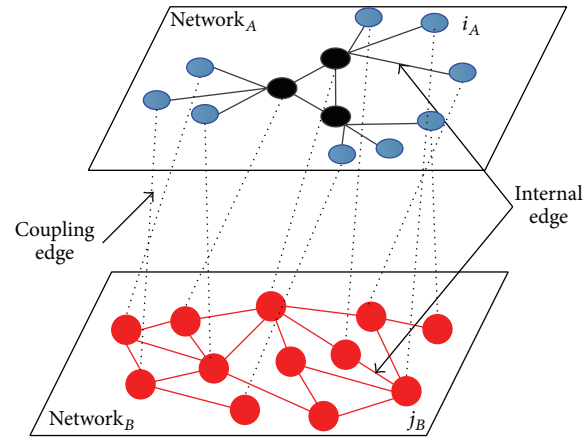

Figure 1: Model of asymmetrical interdependent networks, in which two subnetworks are partly coupled together with proportion p_1. The solid lines in Network$_A$ and Network$_B$ represent the internal edges, while the dashed lines connecting the two subnetworks represent the coupling edges.

The hierarchical structure is established as follows. Firstly, we establish a fully connected top level, the level marker is set to $h = 1$, the number of nodes is n_1, and the edge weight is ω_1. Then, each node in top level establishes relations with M subordinate nodes from the next level, where the level marker is set to $h = 2$. Nodes in this level do not connect with each other. We repeat the former step until $h = H$; then, Network$_A$ with hierarchical weight is completed. The weight of edges connecting level h and level $h + 1$ is set to

$$\omega_{h,h+1} = \omega_1 - C \cdot (h - 1), \tag{2}$$

where constant C controls the weightiness of internal edges which connect neighboring levels.

Network$_B$ is evolved by the rule of WS small-world network because small-world network yields the shortest and most effective paths [32]. The weight of each internal edge is equivalent. It turns from regular network to random network by adjusting the reconnecting probability $p_2 \in [0, 1]$, where $p_2 = 0$ corresponds to the case of nearest-neighbor coupled network; the nodes are placed on a ring lattice with periodic boundary conditions and each node is initially connected to K nearest neighbors. When $p_2 \in (0, 1)$, the WS small-world network model is created by rewiring a small fraction of the links with probability p_2 to nodes chosen at random. The average degree of node is still K. When $p_2 = 1$, it corresponds to a completely random network.

The coupling proportion is set to $p_1 = 0.7$ between Network$_A$ and Network$_B$. The sizes of the subnetworks are set to $N_A = N_B = 340$. In Network$_A$, $M = 4$, $H = 4$, and $n_1 = 4$, so the numbers of subordinate nodes in the next three levels are 16, 64, and 256. Because $C = 2$ and $\omega_1 = 10$, the weights

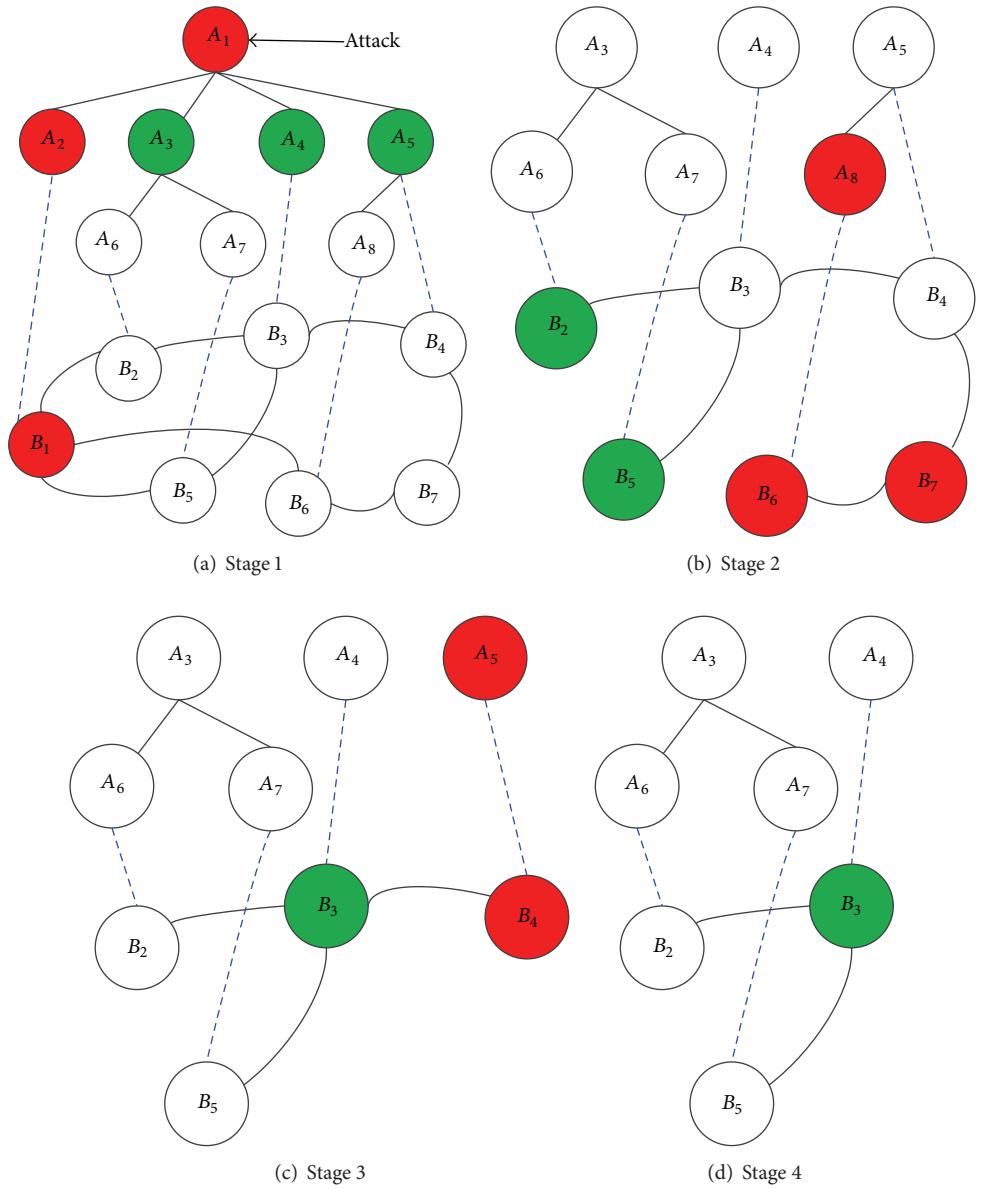

FIGURE 2: The cascading failure under node attack on asymmetrical interdependent network. The initial topology of the asymmetrical network, shown in (a), has a set of nodes in Network$_A$ and Network$_B$, labeled as $\{A_1, A_2, \ldots, A_8\}$ and $\{B_1, B_2, \ldots, B_7\}$, respectively. The internal edges are represented as solid black lines and the coupling edges are represented as dashed blue lines. Red circles represent the failed nodes and green circles represent the nodes that suffered from the load redistribution but are still active.

of internal edges that connect different levels are $\omega_{1,2} = 8$, $\omega_{2,3} = 6$, and $\omega_{3,4} = 4$ according to (2). Network$_B$ is a WS small-world network with $p_2 = 0.1$ and $K = 4$. Due to the randomly "one to one" relationship, we set the weight of coupling edges to be equal to the maximum weight of internal edges connected to the coupled node in Network$_A$.

3. Cascading Failure Model

The coupling property makes the interdependent networks fragile when suffering from intentional attack [16, 18]. Here we focus on the cascading failure of interdependent network induced by load. We define the initial loads $L_i(0)$ of node i as a function of the node intensity s_i:

$$L_i(0) = \lambda s_i^{\alpha}, \tag{3}$$

where load parameters $\lambda > 0$ and $\alpha > 0$ are adjustable to control the distribution of initial load. We can see that each node bears more or less some initial loads according to the node intensity and the loads on each node are a nonlinear function unless the parameter α is equal to 1. ML model [33] conjectures that the capacity of a node is proportional to its

initial loads. There is a linear relationship between capacity C_i of node i and its initial load $L_i(0)$. Consider

$$C_i = (1+\beta)\cdot L_i(0), \tag{4}$$

where $\beta > 0$ is the tolerance parameter. It is well studied that big β leads to excellent robustness. However, considering other perspectives such as cost, the capacity is impossible to be infinite, so it tends to a finite β. In addition, the linear relationship does not fit for many real-world networks, so a nonlinear "load-capacity" model is proposed as follows:

$$C_i = L_i(0) + \beta\cdot L_i(0)^{\theta}, \tag{5}$$

where two tunable parameters $\beta > 0$ and $\theta > 0$ are introduced. If $\theta = 1$, it decays to the linear "load-capacity" model. According to a local nearest redistribution strategy, the proportions of load distribution Π_j and the new added load $\Delta L_{i\to j}$ where the failed node i passes to its neighbor j are as follows[34]:

$$\Pi_j = \frac{C_j}{\sum_{n\in\Gamma_i} C_n},$$
$$\Delta L_{i\to j} = \Pi_j L_i = \frac{C_j}{\sum_{n\in\Gamma_i} C_n} L_i, \tag{6}$$

where n is the neighbor of the failed node i and Γ_i is the set of neighbors which node i connects. If the initial load of node j plus the load that node i transfers to exceeds its capacity ($C_j < L_j + \Delta L_{i\to j}$), node j fails and leads to a new round of load redistribution. The process repeats until there is no overloaded node or the entire network is paralyzed. The evolving procedure is illustrated in Figure 2.

At stage 1 in Figure 2(a), node A_1 is attacked and fails; the load distributes to its neighbors $\{A_2, A_3, A_4, A_5\}$. Node A_2 fails because of overloading and it triggers the failure of B_1 because the load of B_1 exceeds its capacity after receiving some amount of load from A_2. Meanwhile, nodes A_3, A_4, and A_5 are still active because they are not overloaded. At stage 2 in Figure 2(b), due to the load redistribution of node B_1, node B_6 is overloaded, but nodes B_2 and B_5 are still active. B_6 distributes the load to its neighboring nodes which leads to the failure of nodes B_7 and A_8. In this way, the cascading failure propagates in both Network$_A$ and Network$_B$. At stage 3 in Figure 2(c), the failures of nodes B_7 and A_8 trigger the failures of B_4 and A_5. There is no new failure in the interdependent networks in Figure 2(d) and the cascading progress ends at stage 4.

We use R_s to express the relative scale damage caused by node failures:

$$R_s = \frac{S'}{S}, \tag{7}$$

where S (S') is the sum of initial node intensity before (after) node failures.

Similar to the case of node failure, the initial load of edge $L_{ij}(0)$ is related to the node intensities of i and j, as defined in (8). The "load-capacity" model of edges can be expressed in (9). Figure 3 shows the load redistribution rule for edge failure. Consider

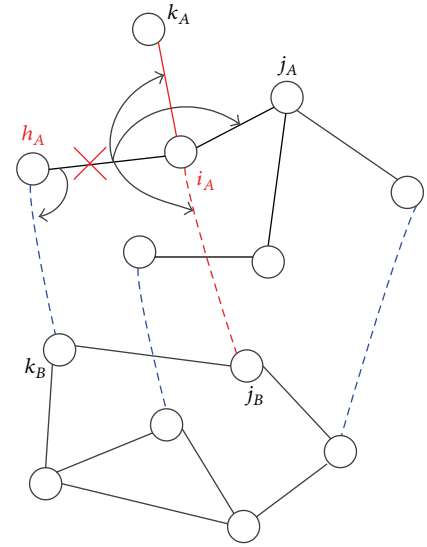

FIGURE 3: The load redistribution triggered by an edge failure. The internal edges are represented as solid black lines, while the coupling edges are represented as dashed blue lines. The black arrowed lines represent the directions of load redistribution from the failed edge and the red solid line represents the edge which is overloaded.

$$L_{ij}(0) = (s_i\cdot s_j)^{\gamma}, \tag{8}$$

where $\gamma > 0$ is a tunable parameter to control initial load of edges. Consider

$$C_{ij} = L_{ij}(0) + \beta\cdot L_{ij}(0)^{\theta}. \tag{9}$$

If a single internal edge $e_{i_A h_A}$ in Network$_A$ fails, the load on the broken edge will be redistributed bidirectionally to its neighboring internal and coupling edges. If the load on neighboring edges plus the extra load exceeds their capacity, this may trigger a recursive process of cascading failures, such as internal edge $e_{i_A k_A}$ and internal edge $e_{i_A j_B}$ shown in Figure 3. After coupling edge $e_{i_A j_B}$ fails, its load proportionally is reassigned to neighboring edges connected to node i_A in Network$_A$ and node j_B in Network$_B$. Consider

$$\Delta L_{i_A\to j_A} = \frac{C_{i_A j_A}}{\sum_{a\in\Gamma_{i_A}} C_{i_A a} + \sum_{b\in\Gamma_{j_B}} C_{j_B b} - 2C_{i_A j_B}} L_{i_A j_B},$$
$$\Delta L_{j_B\to k_B} = \frac{C_{j_B k_B}}{\sum_{a\in\Gamma_{i_A}} C_{i_A a} + \sum_{b\in\Gamma_{j_B}} C_{j_B b} - 2C_{i_A j_B}} L_{i_A j_B}, \tag{10}$$

where Γ_{i_A} (Γ_{j_B}) is the set of neighbors of node i_A (j_B) and $L_{i_A j_B}$ is the initial load of edge $e_{i_A j_B}$. $\Delta L_{i_A\to j_A}$ is the additional load distributed to edge $e_{i_A j_A}$. $\Delta L_{j_B\to k_B}$ is the additional load distributed to edge $e_{j_B k_B}$. Only if $C_{mn} > L_{mn} + \Delta L_{m\to n}$ for any edge will there be no new edge failure in the system.

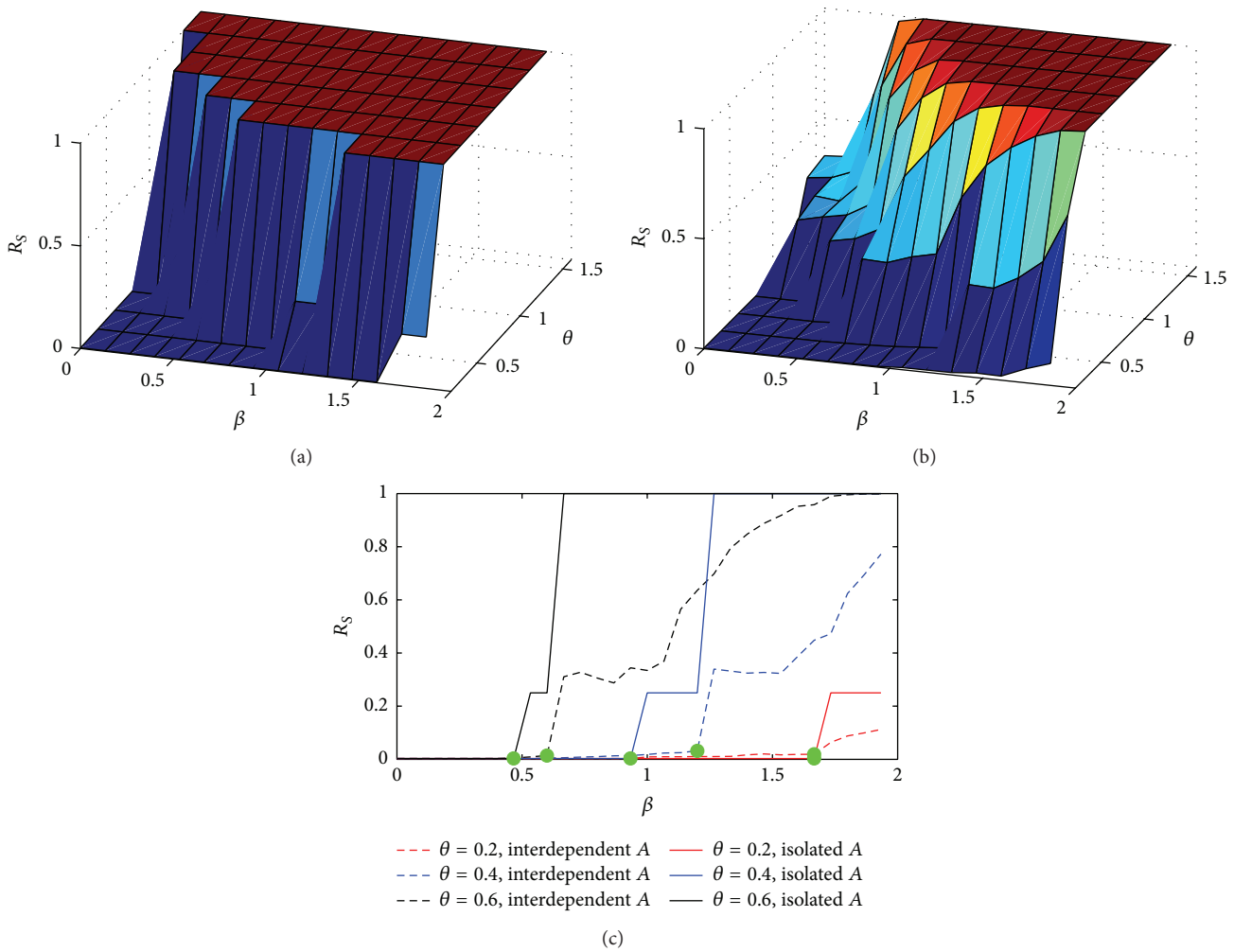

FIGURE 4: The relationship between capacity and robustness of Network$_A$ under node intentional attack. (a) Network$_A$ in isolated status. (b) Network$_A$ in interdependent status. (c) A comparison of Network$_A$ in both isolated status and interdependent status. Capacity parameters $\beta \in [0, 2)$ and $\theta \in [0.2, 1.6]$. Load parameter $\alpha = 0.8$. In (c), the critical value β_C is labeled with green dot. The solid lines denote the isolated status, while the dashed lines denote the interdependent status. Simulation results are averaged over 1000 independent trials.

We finally adopt the relative size of removed edge as R to describe the network robustness under edge attack:

$$R = \sum_{ij} \frac{E_{ij}}{E}, \tag{11}$$

where E_{ij} is the number of failed edges due to cascading failure after e_{ij} is cut off, while E is the total number of edges in the whole system before cascading failures.

4. Results and Discussion

4.1. Analysis of Network Robustness under Node Attack. A similar phenomenon of the isolated status and interdependent status is that R_S has positive relations with the capacity parameters β and θ. This means that high capacity benefits the robustness of Network$_A$. Additionally, it is notable that the curve of R_S abruptly emerges when β approaches a critical value in Figure 4(a), and then it rapidly grows to 1; but, in Figure 4(b), after its abrupt emergence, the robustness indicator then shows a slow increase to 1. In order to find the detailed difference between the two statuses, we fix θ at 0.2, 0.4, and 0.6 separately to compare the curves of R_S in isolated status and interdependent status in Figure 4(c). It can be seen that the solid lines are above the corresponding dashed ones because the interdependent relationship leads to a weaker robustness of Network$_A$. Furthermore, the robustness indicator R_S in isolated status undergoes a short "plateau" state before it grows to 1. In comparison, in the interdependent status, the robustness undergoes a hybrid phase transition.

The robustness of Network$_A$ has a positive relation with the capacity parameter β in Figure 5. However, it has a negative relationship with load parameter α as shown in Figures 5(a) and 5(b). We fix α at 1.2, 1.4, and 1.6 separately to compare the changes of robustness in both statuses. We also find that the robustness of Network$_A$ in isolated status is better than that in interdependent status. In addition, the trend of each curve in Figure 5(c) is similar to that in Figure 4(c).

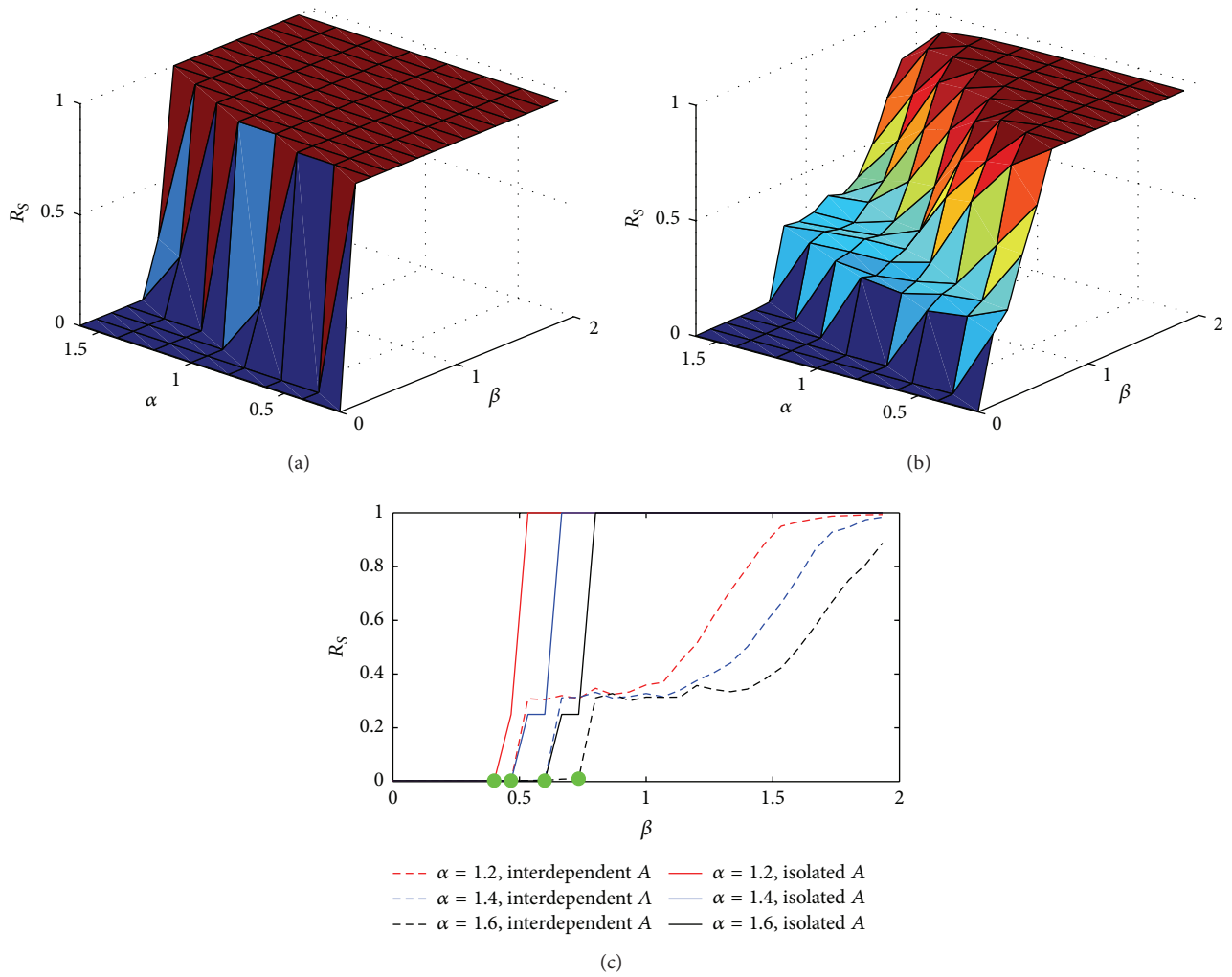

FIGURE 5: The relationship between load and robustness of Network$_A$ under node intentional attack. (a) Network$_A$ in isolated status. (b) Network$_A$ in interdependent status. (c) A comparison of Network$_A$ in both isolated status and interdependent status. Capacity parameters $\beta \in [0, 2)$ and $\theta = 0.8$. The critical value β_C is labeled with green dot. The solid lines denote the robustness of Network$_A$ in isolated status, while the dashed lines denote the robustness of Network$_A$ in interdependent status. Simulation results are averaged over 1000 independent trials.

Because of the hierarchical weight structure in Network$_A$, nodes from the same level have equal initial load and capacity according to (1) and (3). If a node fails, the proportion of load redistribution is divided by the level to which the neighboring nodes belong. The failure probabilities of neighboring nodes from the same level are equivalent, while those of the nodes from different levels are not. That finally leads to the sharp change of R_S when most neighbors fail or the short plateau without large scale of failures in the neighborhood. The hierarchical weight structure in Network$_A$ also leads to a cascade of failures in the isolated status unlike a regular first-order phase transition. Meanwhile, the interdependent relationship leads to the failures from a first-order phase transition to a second-order phase transition.

4.2. Analysis of Network Robustness under Edge Attack. When the edge with maximum initial load $\max(L_{ij}(0))$ in Network$_A$ suffers from intentional attack, the relationship among load, capacity, and robustness is analyzed based on the results in Figures 6 and 7. Under edge attack, the robustness indicator R also shows positive correlations with the capacity parameters β and θ but a negative correlation with load parameter γ. The results shown in Figures 6 and 7 also prove that the robustness can be enhanced by high capacity as well as low initial load. As shown in Figures 6(a) and 6(b) and Figures 7(a) and 7(b), the enhancement of robustness is more prompt in isolated status than in interdependent status. In Figures 6(c) and 7(c), the solid line denoting each value of θ and γ is above the corresponding dashed ones which also indicates a weaker robustness of Network$_A$ in interdependent status. The hierarchical weight structure in Network$_A$ also leads to a plateau on the curves of R in Figure 7(c). Because the initial load and capacity of internal edge L_{ij} which connect the neighboring levels are equal, according to (1), (2), and

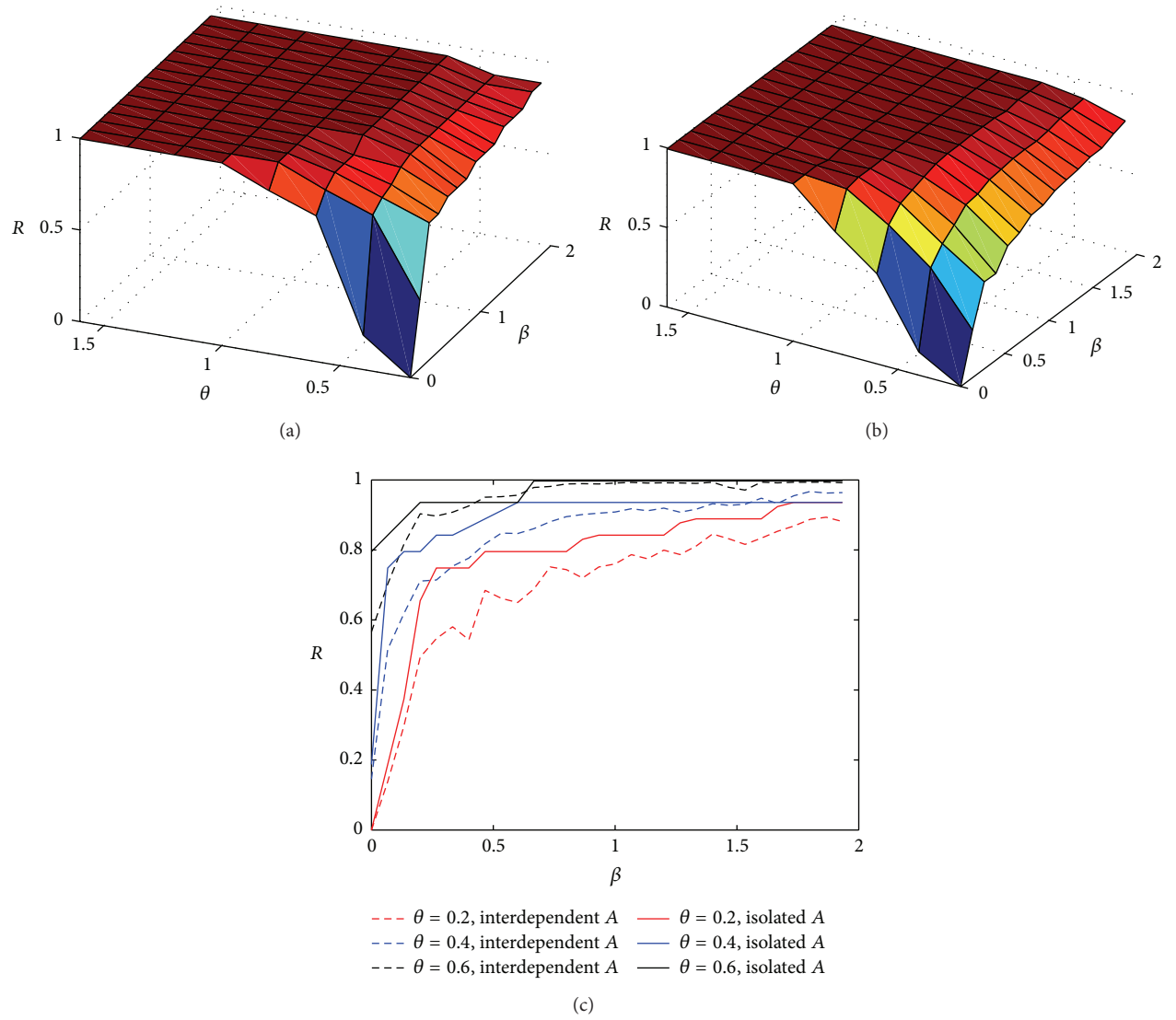

FIGURE 6: The relationship between capacity and robustness of Network$_A$ under edge intentional attack. (a) Network$_A$ in isolated status. (b) Network$_A$ in interdependent status. (c) A comparison of Network$_A$ in both isolated status and interdependent status. Capacity parameters $\beta \in [0, 2)$ and $\theta \in [0.2, 1.6]$. Load parameter $\gamma = 0.8$. The solid lines denote the isolated status, while the dashed lines denote the interdependent status. Simulation results are averaged over 1000 independent trials.

(8). Edges connecting the neighboring levels have equal initial load and capacity. If one internal edge fails, the failure probabilities of edges connecting the same neighboring levels are equivalent, while those of the edges connecting different levels are not. So it leads to the sharp change of R when most edges fail or the plateau without large scale of edge failures.

4.3. Comparison of Asymmetrical and Symmetrical Models. We compare between robustness of the asymmetrical network model we propose and that of a symmetrical network model (WS-WS). The configuration of WS subnets in the symmetrical network model is the same as that of the WS subnet in the asymmetrical network model. The robustness of network under different initial conditions is shown in Figures 8 and 9.

We test intentional node attacks on the studied models under two initial conditions in Figure 8. It can be seen that the robustness of the symmetrical model is stronger than that of the asymmetric model. Additionally, no matter in the symmetrical or the asymmetrical case, the robust levels of Network$_A$ and Network$_B$ under the same conditions are very close to one another.

Additionally, we test intentional edge attacks on the two models under different initial conditions in Figure 9. Similar to the cases on node attack, the robust levels in the symmetrical model are better than those in the asymmetric model. However, what is notable is that $R - \beta$ curves of each subnetwork in the asymmetrical model deviate from each other, while those of the symmetrical model remain resemblant. Network$_A$ is less vulnerable than Network$_B$.

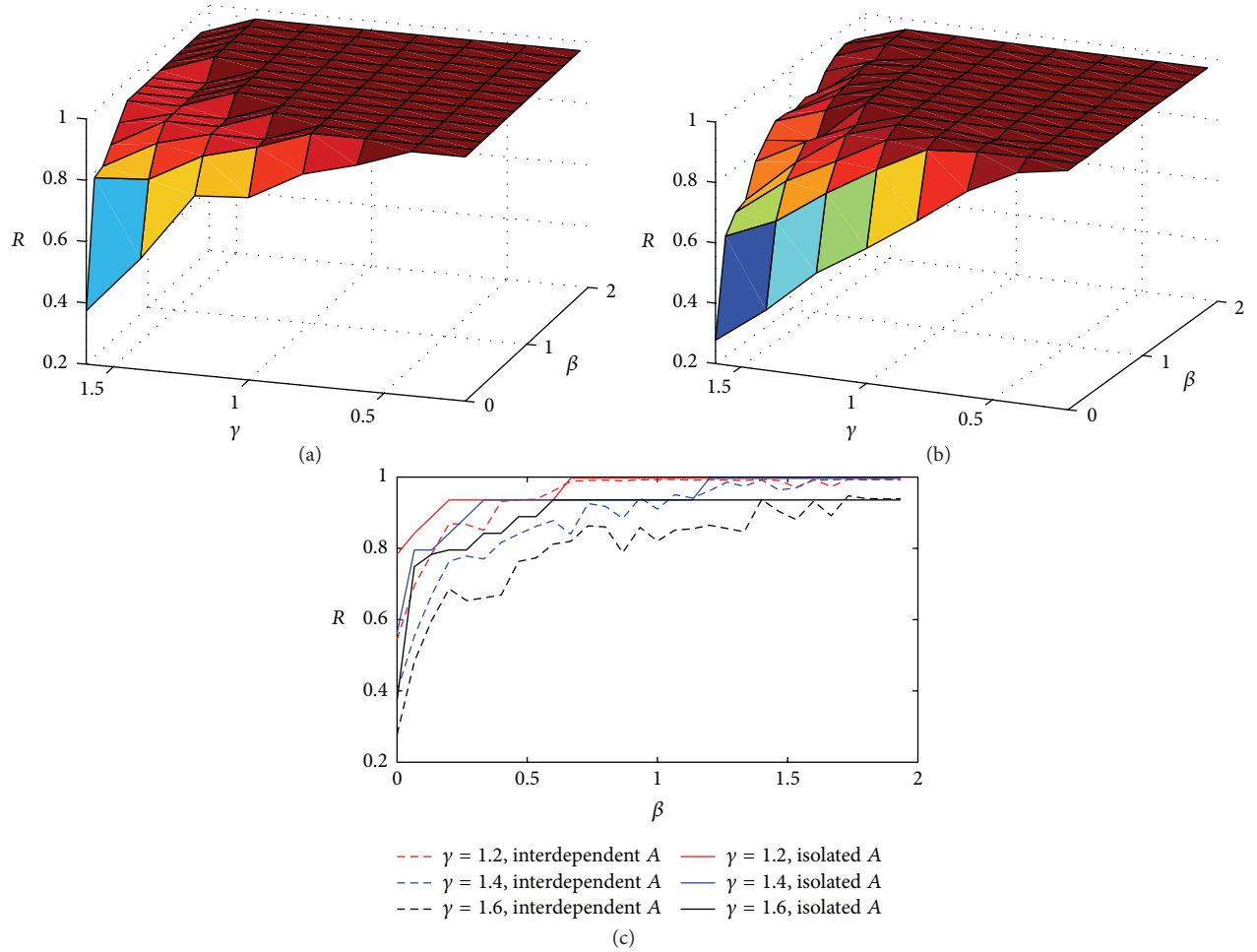

FIGURE 7: The relationship between load and robustness under edge intentional attack in isolated status (a) and in interdependent status (b). (c) A comparison of Network$_A$ in both isolated status and interdependent status. Capacity parameters $\beta \in [0, 2)$ and $\gamma \in [0.2, 1.6]$. Capacity parameter $\theta = 0.8$. The solid lines denote the robustness of Network$_A$ in isolated status, while the dashed lines denote the robustness of Network$_A$ in interdependent status. Simulation results are averaged over 1000 independent trials.

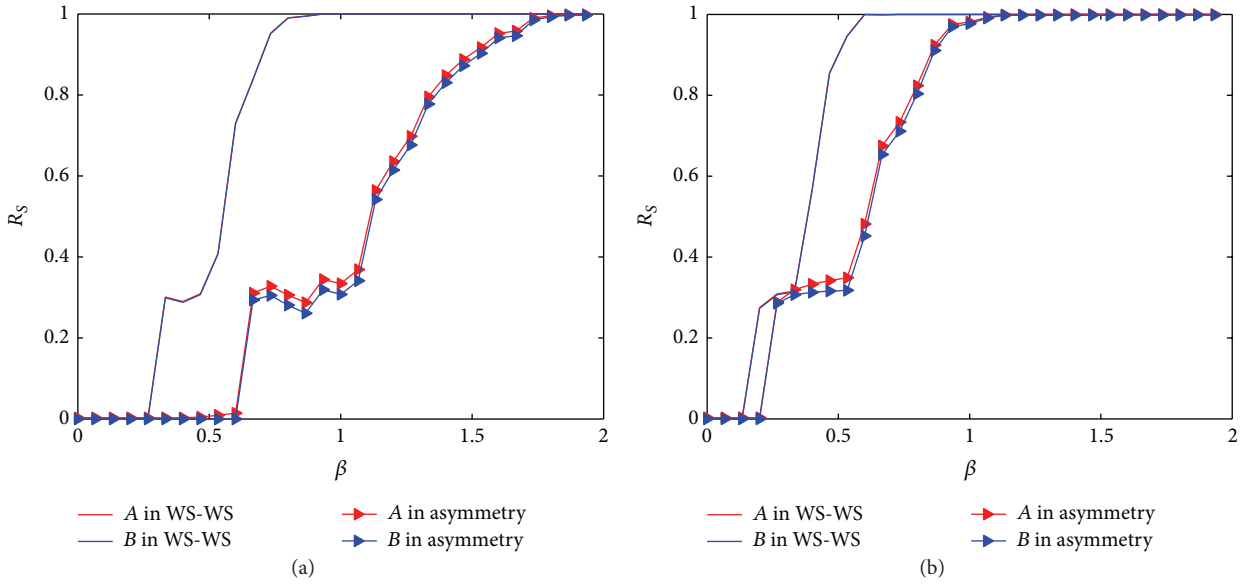

FIGURE 8: Comparison of node attack in symmetrical and asymmetrical network models under different initial conditions. (a) $\alpha = 0.8$ and $\theta = 0.6$. (b) $\alpha = 0.6$ and $\theta = 0.8$. The red lines without triangles denote the robustness in WS-WS network model, while solid lines with triangles denote the robustness in Network$_B$. Simulation results are averaged over 1000 independent trials.

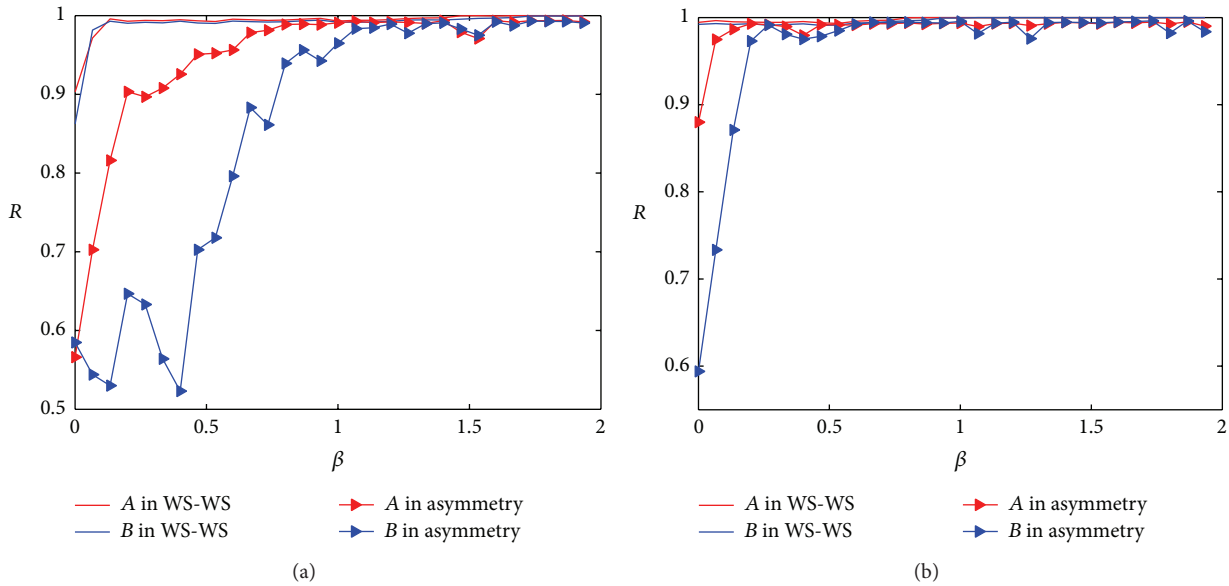

FIGURE 9: Comparison of edge attack in symmetrical and asymmetrical network models under different initial conditions. (a) $\gamma = 0.8$ and $\theta = 0.6$. (b) $\gamma = 0.6$ and $\theta = 0.8$. The red lines without triangles denote the robustness in WS-WS network model, while solid lines with triangles denote the robustness in Network$_B$. Simulation results are averaged over 1000 independent trials.

5. Conclusion

Interdependent network is a representative abstraction of realistic systems, where failures in one system may trigger a cascade of failures in the other system through interactions among systems. For instance, load redistribution caused by node or edge failures in one subnetwork may trigger an iterative progress of cascading failure in interdependent networks. In this paper, firstly, we propose an interdependent network model considering asymmetrical property of the two subnetworks. Secondly, a nonlinear "load-capacity" model is also proposed for nodes and edges, respectively, to model the cascading failures. Thirdly, we conduct a systematic series of experiments to analyze the robustness of interdependent network under attack and make comparisons with the situation of well-studied symmetrical WS-WS network model. (1) Interdependent networks are more fragile compared with isolated ones. (2) The hierarchical weight structure leads to a short "plateau" phenomenon in isolated status unlike the regular first-order phase transition in nonhierarchical isolated networks. Under node attack, only if the capacity reaches a critical value β_C can the robustness abruptly emerge and rapidly approach 1. Furthermore, the interconnections lead to the robustness curve from a first-order phase transition to a second-order phase transition in interdependent networks. (3) Under edge attack, the hierarchical weight structure also causes a plateau in an iterative process of cascading failures in isolated status. The change of robustness in isolated network is more prompt than that in interdependent network. (4) Compared with symmetrical WS-WS network model, the robustness of the asymmetrical model is weaker. Under node attack, no matter in the symmetrical or the asymmetrical case, the two subnetworks have similar robustness. However, under edge attack, subnetworks in the asymmetrical model perform differently, while those of the symmetrical model remain resemblant.

Conflict of Interests

The authors declare that there is no conflict of interests regarding the publication of this paper.

Authors' Contribution

Haiyan Han planned the work, implemented the experiment, and drafted the main part of the paper. Rennong Yang contributed to the error analysis.

Acknowledgments

The work described in this paper is supported by the Twelfth Five-Year Plan Pre-Research Project (no. 402040401) and Science and Technology Research and Development Project of Shaanxi Province (no. 2013kjxx-82).

References

[1] R. Albert, H. Jeong, and A.-L. Barabási, "Error and attack tolerance of complex networks," *Nature*, vol. 406, no. 6794, pp. 378–382, 2000.

[2] C. M. Schneider, A. A. Moreira, J. S. Andrade Jr., S. Havlin, and H. J. Herrmann, "Mitigation of malicious attacks on networks," *Proceedings of the National Academy of Sciences of the United States of America*, vol. 108, no. 10, pp. 3838–3841, 2011.

[3] G. Li, S. D. S. Reis, A. A. Moreira et al., "Towards design principles for optimal transport networks," *Physical Review Letters*, vol. 104, no. 1, Article ID 018701, 4 pages, 2010.

[4] J. Zhao, H. Zhou, B. Chen, and P. Li, "Research on the structural characteristics of transmission grid based on complex network theory," *Journal of Applied Mathematics*, vol. 2014, Article ID 261798, 12 pages, 2014.

[5] J. Gao, S. V. Buldyrev, H. E. Stanley, and S. Havlin, "Networks formed from interdependent networks," *Nature Physics*, vol. 8, no. 1, pp. 40–48, 2012.

[6] L. Zhang, J. Cao, and J. Li, "Complex networks: statistical properties, community structure, and evolution," *Mathematical Problems in Engineering*, vol. 2015, Article ID 590794, 7 pages, 2015.

[7] A. Bashan, R. Parshani, and S. Havlin, "Percolation in networks composed of connectivity and dependency links," *Physical Review E—Statistical, Nonlinear, and Soft Matter Physics*, vol. 83, no. 5, Article ID 051127, 8 pages, 2011.

[8] S. Funk and V. A. A. Jansen, "Interacting epidemics on overlay networks," *Physical Review E*, vol. 81, no. 3, Article ID 036118, 10 pages, 2010.

[9] M. D. Santos, S. N. Dorogovtsev, and J. F. Mendes, "Biased imitation in coupled evolutionary games in interdependent networks," *Scientific Reports*, vol. 4, pp. 4436–4439, 2014.

[10] C. D. Brummitt, R. M. D'Souza, and E. A. Leicht, "Suppressing cascades of load in interdependent networks," *Proceedings of the National Academy of Sciences of the United States of America*, vol. 109, no. 12, pp. E680–E689, 2012.

[11] C. M. Schneider, N. Yazdani, N. A. M. Araújo, S. Havlin, and H. J. Herrmann, "Towards designing robust coupled networks," *Scientific Reports*, vol. 3, pp. 1969–1972, 2013.

[12] R. Parshani, S. V. Buldyrev, and S. Havlin, "Critical effect of dependency groups on the function of networks," *Proceedings of the National Academy of Sciences of the United States of America*, vol. 108, no. 3, pp. 1007–1010, 2011.

[13] J. Shao, S. V. Buldyrev, S. Havlin, and H. E. Stanley, "Cascade of failures in coupled network systems with multiple support-dependence relations," *Physical Review E*, vol. 83, no. 3, Article ID 036116, 9 pages, 2011.

[14] S. V. Buldyrev, R. Parshani, G. Paul, H. E. Stanley, and S. Havlin, "Catastrophic cascade of failures in interdependent networks," *Nature*, vol. 464, no. 7291, pp. 1025–1028, 2010.

[15] Y. Hu, B. Ksherim, R. Cohen, and S. Havlin, "Percolation in interdependent and interconnected networks: abrupt change from second- to first-order transitions," *Physical Review E*, vol. 84, Article ID 066116, 6 pages, 2011.

[16] X. Huang, J. Gao, S. V. Buldyrev, S. Havlin, and H. E. Stanley, "Robustness of interdependent networks under targeted attack," *Physical Review E—Statistical, Nonlinear, and Soft Matter Physics*, vol. 83, no. 6, Article ID 065101, 4 pages, 2011.

[17] J. Gao, S. V. Buldyrev, S. Havlin, and H. E. Stanley, "Robustness of a network formed by n interdependent networks with a one-to-one correspondence of dependent nodes," *Physical Review E*, vol. 85, no. 6, Article ID 066134, 13 pages, 2012.

[18] G. Dong, J. Gao, R. Du et al., "Robustness of network of networks under targeted attack," *Physical Review E*, vol. 87, Article ID 052804, 7 pages, 2013.

[19] R. Parshani, S. V. Buldyrev, and S. Havlin, "Interdependent networks: reducing the coupling strength leads to a change from a first to second order percolation transition," *Physical Review Letters*, vol. 105, Article ID 048701, 4 pages, 2010.

[20] P. Erdös and A. Rényi, "On the evolution of random graphs," *Publications of the Mathematical Institute of the Hungarian Academy of Sciences Series A*, vol. 5, pp. 17–61, 1960.

[21] D. J. Watts and S. H. Strogatz, "Collective dynamics of 'small-world' networks," *Nature*, vol. 393, no. 6684, pp. 440–442, 1998.

[22] A. L. Barabási and R. Albert, "Emergence of scaling in random networks," *Science*, vol. 286, no. 5439, pp. 509–512, 1999.

[23] S. M. Chen, X. Q. Zou, H. Lü, and Q. G. Xu, "Research on robustness of interdependent network for suppressing cascading failure," *Acta Physica Sinica*, vol. 63, no. 2, Article ID 028902, 10 pages, 2014.

[24] M. Gong and L. Ma, "Enhancing robustness of coupled networks under targeted recoveries," *Science Report*, vol. 5, Article ID 8439, 7 pages, 2015.

[25] Z. D. Zhao, Y. Liu, and M. Tang, "Epidemic variability in hierarchical geographical networks with human activity patterns," *Chaos*, vol. 22, no. 2, Article ID 023150, 7 pages, 2012.

[26] J. McNerney, B. D. Fath, and G. Silverberg, "Network structure of inter-industry flows," *Physica A*, vol. 392, no. 24, pp. 6427–6441, 2013.

[27] L. P. Chi, R. Wang, H. Su et al., "Structural properties of US flight network," *Chinese Physics Letter*, vol. 20, no. 8, pp. 1393–1396, 2003.

[28] I. B. Utne, P. Hokstad, and J. Vatn, "A method for risk modeling of interdependencies in critical infrastructures," *Reliability Engineering & System Safety*, vol. 96, no. 6, pp. 671–678, 2011.

[29] G. Fu, R. Dawson, M. Khoury, and S. Bullock, "Interdependent networks: vulnerability analysis and strategies to limit cascading failure," *The European Physical Journal B*, vol. 87, article 148, 10 pages, 2014.

[30] M. Khoury, S. Bullock, G. Fu, and R. Dawson, "Improving measures of topological robustness in networks of networks and suggestion of a novel way to counter both failure propagation and isolation," *Infrastructure Complexity*, vol. 2, article 1, 20 pages, 2015.

[31] S. D. Li, L. Li, Y. Jia, X. Liu, and Y. Yang, "Identifying vulnerable nodes of complex networks in cascading failures induced by node-based attacks," *Mathematical Problems in Engineering*, vol. 2013, Article ID 938398, 10 pages, 2013.

[32] L. Lü, D.-B. Chen, and T. Zhou, "The small world yields the most effective information spreading," *New Journal of Physics*, vol. 13, Article ID 123005, 6 pages, 2011.

[33] A. E. Motter, "Cascade control and defense in complex networks," *Physical Review Letters*, vol. 93, no. 9, Article ID ID098701, 4 pages, 2004.

[34] X. Z. Peng, H. Yao, J. Du, Z. Wang, and C. Ding, "Invulnerability of scale-free network against critical node failures based on a renewed cascading failure model," *Physica A: Statistical Mechanics and its Applications*, vol. 421, pp. 69–77, 2015.